Journal of Mines, Metals and Fuels, *71(12C) : 322-331; 2023. DOI: 10.18311/jmmf/2023/47259*

Print ISSN : 0022-2755

Journal of Mines, Metals and Fuels

Contents available at: *www.informaticsjournals.com/index.php/jmmf*

Impact of Drag Force, Dufour and Suction/Blowing on 2D Radiated Viscous Nanomaterial over Unsteady Stretching Surface

R. Sumithra[1], P. A. Dinesh[2], Sweeti Yadav[2], K. R. Roopa[2], G. K. Kalavathi[3], G. S. Ashoka[1], D. Prabhakar[1], R. B. Sandhya[1] and Vinod[1]

[1]Department of Mathematics, Nrupathunga University, Bengaluru – 560001, Karnataka, India; sumitradiya@yahoo.com, ashokgs2001@gmail.com, dprabhakar7483@gmail.com, sandhya2000rb@gmail.com, vinodharsoor@gmail.com
[2]Department of Mathematics, M S Ramaiah Institute of Technology, Bengaluru – 560054, Karnataka, India; dineshdpa@msrit.edu, sweetiyadav1989@gmail.com, krroopa870@gmail.com
[3]Department of Mathematics, Malnad College of Engineering, Hassan – 573202, Karnataka, India; gkk@mcehassan.ac.in

Abstract

Numerical analysis of radiated viscous nanomaterial by a stretching surface with drag force, dofour effect and Joule heat source is presented in current research. With suitable method the partial differential equation is changed into a system of ordinary differential equations. Numerical solution of resultant equation is obtained by RKF45 technique. The effect of various relevant factors on velocities, concentration, temperature, Nusselt number is determined, and demonstrations are provided through the use of figures and tables. The obtained findings are compared to the previously obtained results. Major findings of this research are heat trasfer rate increases under the influence of dufour effect while it decline with drag force and suction/blowing effect. The results are impactful in various industries application like nuclear reactors, synthetic textiles, metal extrusion, crystal growth etc.

Keywords: *Dufour Effect, Nanomaterials, Suction/Blowing*

1.0 Introduction

Nanomaterials are materials with a single unit size ranging from 1 to 100 nm. Special optical, electrical, thermophysical, or mechanical properties are typically found in nanoscale materials. Nanomaterials are increasingly becoming more commercialized and widespread. The rheology of nanofluids is studied by various researchers. Sakidis[1] was the first to investigate fluid flow in a continuous solid surface in comparison to a surface having a finite length. He discovered that the differential boundary layer equation is appropriate, as long as the boundary layer conditions differ in both situations. Crane[2] builds on Sakiadis' work by studying fluid flow across an extended plate with velocity related to its separation from slit. Since the development of the word by Choi[3] scientific study of nanofluids has grown at an exponential rate. His research demonstrates the improvement of the heat conductivity of these tiny fluids in the creation and use of Newtonian fluids. Buongiorno[4] investigated the key variables of the diffusion of Brownian particles and thermophoresis dispersion in nanofluid transport. Various scholars continued this study in other fields such as MHD, permeable surfaces, nonlinear

**Author for correspondence*

electromagnetic radiation, viscous disintegration, heat production, chemical processes, and Arrhenius energy.

Many real-world situations include the flow of boundary layers induced by stretchy sheets. It has several uses such as hot rolling, paper manufacture, condensed process, artificial fibres, and so on. It is possible for the stretching surface to be straight or complex. Crane[5] was the first to investigate the linear stretching surface, while Khan and Pop[6] investigated the nonlinear stretching surface. This study on the convective condition of the boundary is extended by Makinde and Aziz[7]. Cortell[8] was the first to investigate the movement of the boundary layer by an irregularly extending sheet in the presence of heat radiation and viscous dissipation. Heat transport in a non-isothermal stretched sheet was investigated by Prasad *et al.*[9] and Mukhopadhyay[10]. Srinvasulu and Bandari[11] investigated the Arrhenius equation and a heat source via a nonlinearly stretched plate. MHD radiative nanofluid flow in a porous media caused by a nonlinear stretching sheet by Jafar *et al.*[12]. The thermal and mass transmission of an electrically charged incompressible nanofluid across a heated stretched sheet due to a convective boundary layer is addressed in this work. Elgazery[13] investigated flows over an uneven stretched surface with a heat source/sink in an angled magnetic field. Nonlinear stretchable sheets in pore-filled materials were investigated by Jafar *et al.*[14]. Thin layer nanofluid on an angled stretching surface was investigated by Saeed *et al.*[15]. Rasool *et al.*[16] used a nonlinear extending surface to simulate nanofluid flow with convection as a boundary condition. The heat transfer characteristics and thermal slip of nanofluid mixtures over porous, irregular, curve-shaped substrates were investigated by Abbas *et al.*[17].

The mass flow caused by concentration variations is known as the Dufour. The Dufour effect has a wide range of uses in the field of chemical engineering and the earth sciences. These effects are typically ignored in heat and mass transfer transit because they have smaller orders of magnitude than the ones given by Fourier and Fick's law, but they have numerous applications in petrology, hydrodynamics, the study of nuclear waste, and so on. Irreversibility analysis in Darcy-Forchheimer flow of viscous fluid with Dufour and Soret effects via finite difference method by a stretched sheet is examined by Khan *et al.*[18]. Energy attribution is discussed through thermodynamic first law with Joule heating, radiation, Lorentz force and dissipation effects. Soret-Dufour and radiative aspects in hydro magnetized nano fluid flow in stratified porous medium is researched by Anwar *et al.*[19]. The findings of the paper are the enhancement in Dufour factor decreases the temperature profile while increase the Soret parameter leads to increase in concentration profile.

The physical action of a current passing through a conductor of electricity producing thermal energy is known as joule heating. Resistance ovens, resistance direct heating, induction heating is some of the applications of joule heating. Joule heating effect and chemical reaction effect on peristaltic transporting on couple-stress micropolar nanofluids in a narrow channel allows for electrokinetic transmission is studied by Reddy[20]. The continuous flow of an incompressible a two-dimensional Oldroyd-B nanofluid across a stretched sheet is examined using magneto-hydrodynamics (MHD) and a medium that is porous with magnetically charged, Joule effect, electrical, and thermal energy effects via investigated by Ullah[21] .

The present study is to investigate the combined effects of drag force, dufour and suction/blowing on 2 D radiated viscous nanofluid over unsteady stretching surface. With suitable method the partial differential equation is changed into a system of ordinary differential equations. Numerical solution of resultant equation is obtained by RKF45 technique. The effect of various relevant factors on velocities, concentration, temperature, Nusselt number is determined, and demonstrations are provided through the use of figures and tables.

2.0 Mathematical Description

Assume a boundary layer nanofluid that flows over a porous stretching material under the effect of a heat source and radiation. The fluid is subsequently electrically transmitted, and the effects of viscosity dissipation, Ohmic, and Joule are not disregarded. Assume that the point of origin is static and the area around it is being extended with velocity along x-axis, temperature, magnetic field and heat source rate. In a direction that is orthogonal to the surface, magnetic field is provided. S is the wall suction/blowing in the vertical direction. Figure 1 depicts the geometrical description of the model's physical structure.

Using the assumptions stated above, the equations of movement, energy, and dispersion generated the following results[22]:

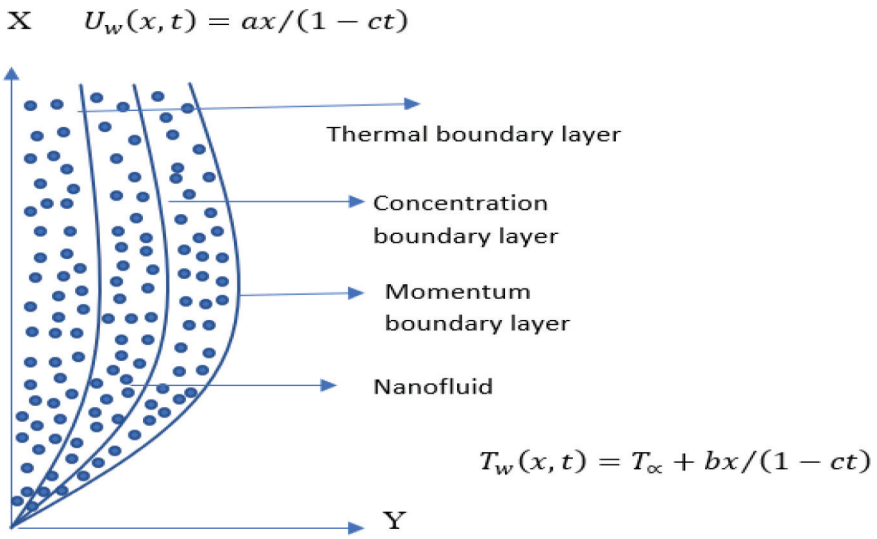


Figure 1. Physical description.

$$\frac{\partial u}{\partial x}+\frac{\partial v}{\partial y}=0 \tag{1}$$

$$\frac{\partial u}{\partial t}+u\frac{\partial u}{\partial x}+v\frac{\partial u}{\partial y}=v\frac{\partial^2 u}{\partial y^2}-\frac{\bar{\mu}}{k\rho_0}u-\frac{\sigma}{\rho}B^2\mathrm{u} \tag{2}$$

$$\begin{aligned}&(\rho c)_f\left(\frac{\partial T}{\partial t}+u\frac{\partial T}{\partial x}+v\frac{\partial T}{\partial y}\right)=k\frac{\partial^2 T}{\partial y^2}\\&+(\rho c)_p\left\{D_B\frac{\partial C}{\partial y}\frac{\partial T}{\partial y}+\frac{D_T}{T_\infty}\left(\frac{\partial T}{\partial y}\right)^2\right\}\\&-\frac{1}{\rho C_p}\frac{\partial q_r}{\partial y}+\frac{D_m}{C_\infty}\left(\frac{\partial^2 c}{\partial y^2}\right)\\&+\frac{\mu}{\rho C_p}\left(\frac{\partial u}{\partial y}\right)^2+\frac{Q_0}{\rho C_p}(T-T_\infty)\end{aligned} \tag{3}$$

$$\frac{\partial C}{\partial t}+u\frac{\partial C}{\partial x}+v\frac{\partial C}{\partial y}=D_B\frac{\partial^2 C}{\partial y^2}+\frac{D_T}{T_\infty}\frac{\partial^2 T}{\partial y^2} \tag{4}$$

Boundary constraints are

$$\begin{aligned}&u(x,0,t)=u_w, v(x,0,t)=v_0, T(x,0,t)\\&=T_W, C(x,0,t)=C_W, u(x,\infty,t)\\&=0, T(x,\infty,t)=T_\infty, C(x,\infty,t)=C_\infty\end{aligned} \tag{5}$$

Here D_m is mass diffusion coefficient, D_b is Brownian motion, D_T is thermophoretic coefficient, $(pc)_p$ is heat capacity of nanoparticle and $(pc)_f$ is heat capacity of fluid.

By Rosseland approximation

$$q_r=-\frac{4\sigma^*\partial T^3}{3k^*\partial y} \tag{6}$$

Expand T^4 using Taylor's series and using (6) we get:

$$\begin{aligned}&(\rho c)_f\left(\frac{\partial T}{\partial t}+u\frac{\partial T}{\partial x}+v\frac{\partial T}{\partial y}\right)=k\left(1+\frac{16\sigma^* T_\infty^{\ 3}}{3k^*}\right)\frac{\partial^2 T}{\partial y^2}\\&+(\rho c_p)\left\{D_B\frac{\partial C}{\partial y}\frac{\partial T}{\partial y}+\frac{D_T}{T_\infty}\left(\frac{\partial T}{\partial y}\right)^2\right\}+\\&+\frac{D_m}{C_\infty}\left(\frac{\partial^2 c}{\partial y^2}\right)+\frac{\mu}{\rho C_p}\left(\frac{\partial u}{\partial y}\right)^2\\&+\frac{Q_0}{\rho C_p}(T-T_\infty)\end{aligned} \tag{7}$$

Non-dimensional numbers assumed are

$$\begin{aligned}&\theta(\eta)=\frac{(T-T_\infty)}{(T_W-T_\infty)}, \varnothing(\eta)=\frac{(C-C_\infty)}{(C_W-C_\infty)},\\&\eta=y\left(\frac{u_w}{vx}\right)^{\frac{1}{2}}, \Psi=\sqrt{u_w vx}f(\eta).\end{aligned} \tag{8}$$

Transformation defined in (8) satisfy equation (1) and equation (2), (4) and (7) takes the form

$$f'''-f'^2+f''f-A\left(\frac{1}{2}\eta f''+f'\right)-(M+\lambda)f'=0 \tag{9}$$

$$A\left(\theta+\frac{1}{2}\eta\theta'\right)+f'\theta-f\theta'=\left(\frac{1+R}{P_r}\right)\theta''$$
$$+N_b\phi'\theta'+N_t\left(\theta'\right)^2+E_c f''^2+\gamma\theta+Du\phi'' \quad (10)$$

$$\frac{1}{Sc}\varnothing''-A(\eta 2^{-1}\varnothing'+\varnothing)+f'\varnothing-f\varnothing'+\frac{Nt}{Nb}\theta''=0 \quad (11)$$

Dimensionless boundary constraints are:

$$f=S, f'=1, \theta=1, \varnothing=1 \ as\,\eta\,tends\,to\,0 \quad (12)$$

$$f'=0, \theta=0, \varnothing=0 \ as\,\eta\,tends\,to\,\infty$$

Non dimensional parameters are

$$A=\frac{c}{a},=\frac{Q_0}{\rho c_p a}, P_r=\frac{\vartheta}{k}, M=\frac{\sigma B_0^2}{\rho a}, EC=\frac{U_w^2}{C_p\left(T_W-T_\infty\right)},$$
$$N_b=\frac{\left(\rho c\right)_p}{\left(\rho c\right)_f}\frac{D_B}{\vartheta}(C_W-C_\infty), N_t=\frac{\left(\rho c\right)_p}{\left(\rho c\right)_f}\frac{D_T}{T_\infty\vartheta}\left(T_W-T_\infty\right),$$
$$\vartheta=\frac{\mu}{\rho}, Sc=\frac{\vartheta}{D_B}, Du=\frac{D_m}{C_\infty\vartheta\left(\rho c\right)_f}\frac{\left(C_W-C_\infty\right)}{\left(T_W-T_\infty\right)}$$

A is Unsteady Parameter, R is Radiation Parameter, M is Magnetic Field Parameter, P_r is Prandtl Number, N_t is Thermophoresis Constraint, N_b is Brownian Motion Constraint, Ec is Eckert Number, Sc is Schimdt Number, S is the suction parameter, Du is dufour effect.

Skin friction coefficient is given as

$0.5 * C_{fx}\,\mathrm{Re}_x^{\frac{1}{2}} = -f''(0)$, Re denotes the local Reynolds number. (13)

Nusselt number is given as

$$Nu_x\,\mathrm{Re}_x^{\frac{-1}{2}} = \theta'(0) \quad (14)$$

3.0 Numerical Procedure

Because these equations are extremely complex and non-linear in nature, they are difficult to solve analytically, hence a numerical approach known as the shooting method followed by the Runge-Kutta method of fourth order is used under the boundary condition.

One approach to resolving this issue is the Runge-Kutta Fehlberg technique (RKF45). It offers a technique for determining whether the correct step size h needs to be utilized. Two distinct approximations for the answer are created and compared at each stage. If two solutions are almost same, the approximation is acceptable.

The step size is adjusted if the two responses differ from one another to a defined accuracy. The value of the step is raised if the solutions agree to a higher number of digits than necessary. Each step size necessitates the usage of the six values listed below.

Then, using a Runge-Kutta approach of order 4, a nearest-neighboring to the solution of the starting value issue is created.

The influence of the porosity parameter on velocities is seen in Figure 2. Because the fluid-particle interaction is reduced, velocity exhibits an inverse relationship with the permeability parameter.

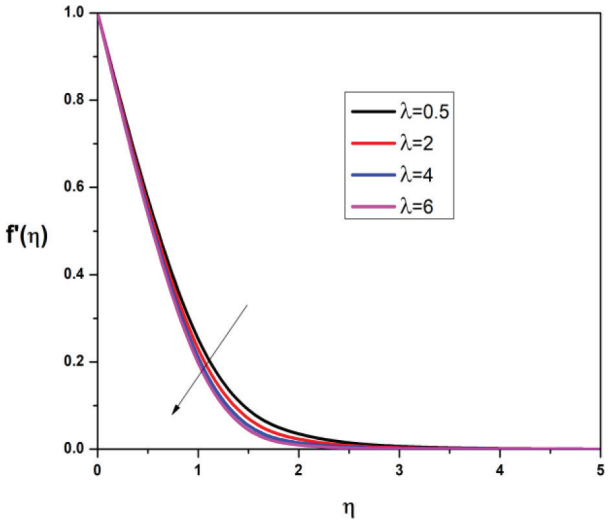


Figure 2. Plot of dimensionless velocity verses drag force.

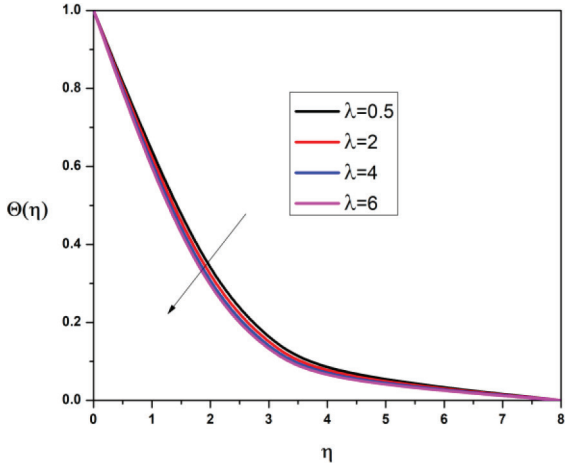


Figure 3. Plot of temperature Θ verses drag force.

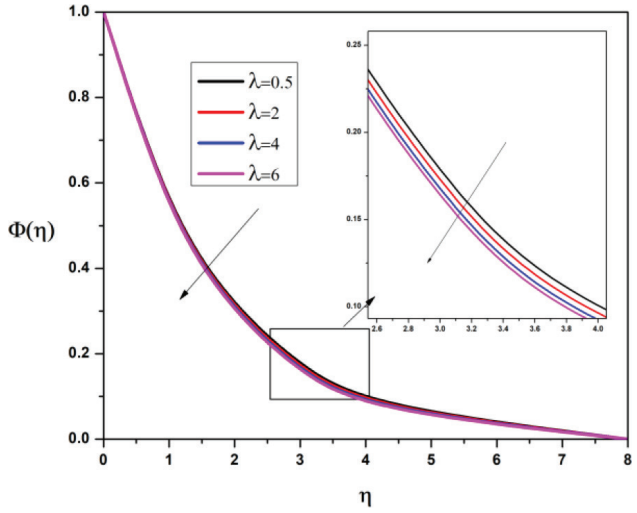


Figure 4. Plot of concentration verses drag force.

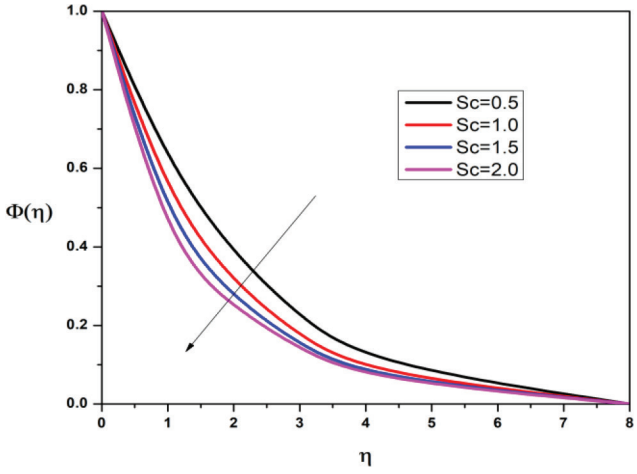


Figure 5. Plot of concentration verses Schmidt number.

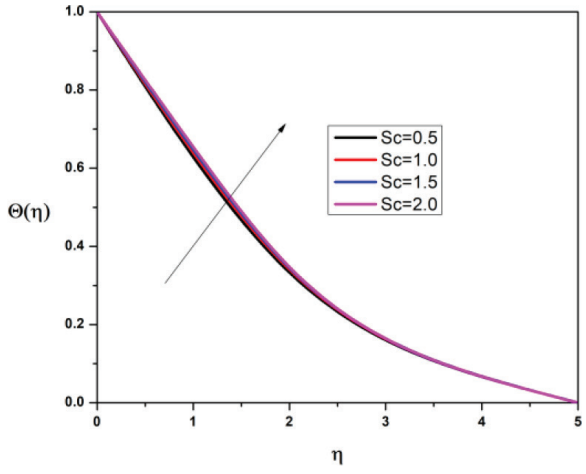


Figure 6. Plot of temperature verses Schmidt number.

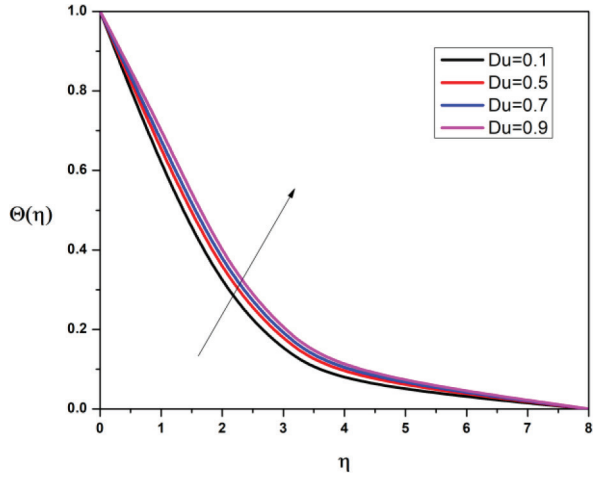


Figure 7. Plot of temperature θ verses Dufour force Du.

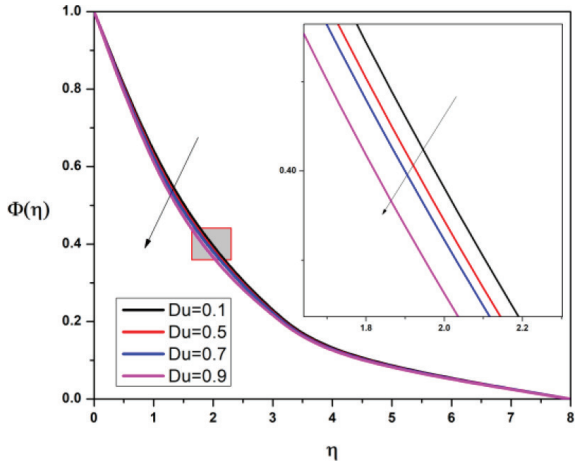


Figure 8. Plot of concentration verses Dufour force Du.

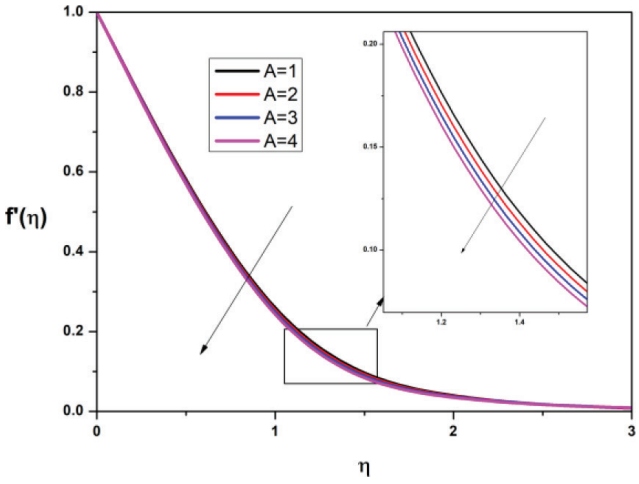


Figure 9. Plot of dimensionless velocity verses unsteady parameter A.

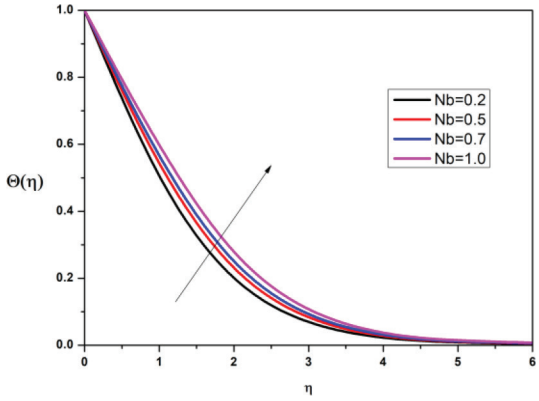


Figure 10. Plot of temperature θ verses Brownian motion constraint N_b.

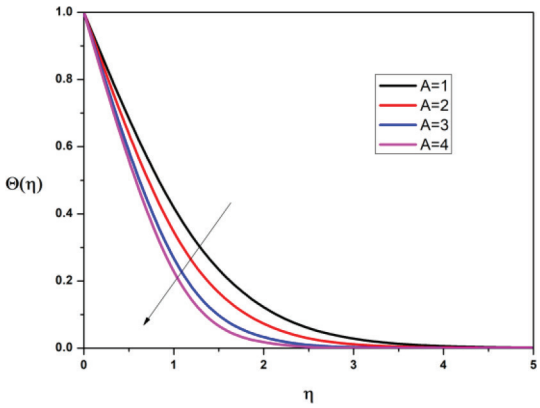


Figure 11. Plot of temperature θ verses unsteady parameter A.

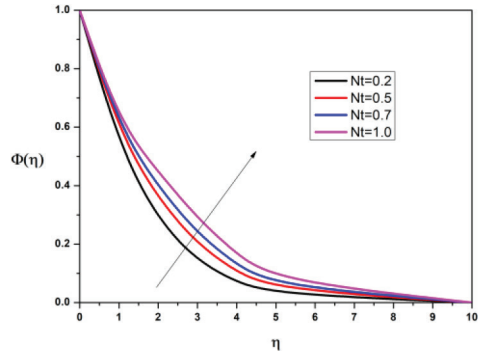


Figure 12. Plot of concentration Φ verses thermophoresis constraint N_t.

The effect of the porosity parameter on temperature is seen in Figure 3. Slow motion causes temperature degradation as a result of the temperature of the thermal boundary layer to decrease as the permeability parameter develops.

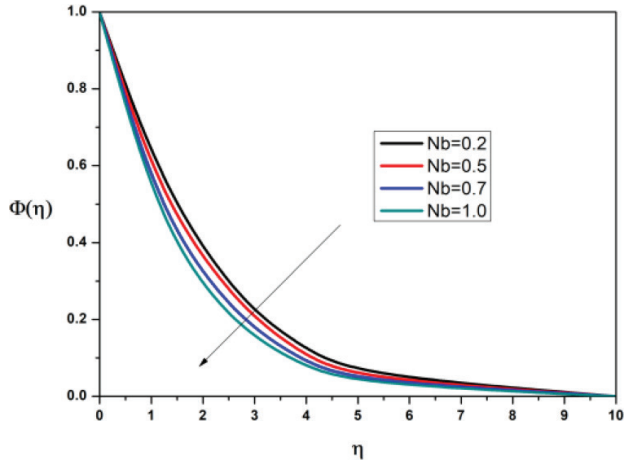


Figure 13. Plot of concentration Φ verses Brownian motion constraint N_b.

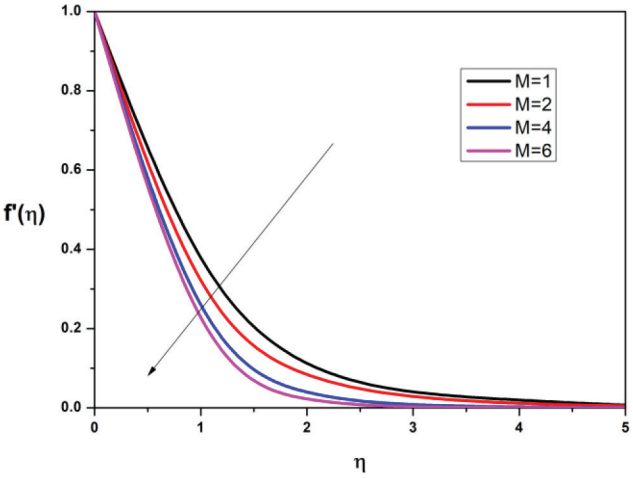


Figure 14. Plot of dimensionless velocity verses Hartmann number M.

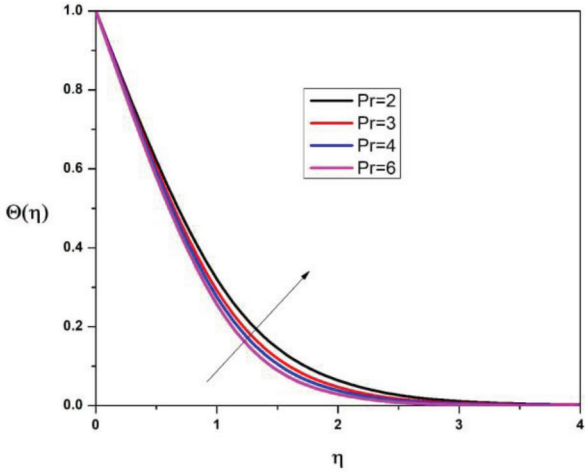


Figure 15. Plot of temperature θ verses Prandtl number Pr.

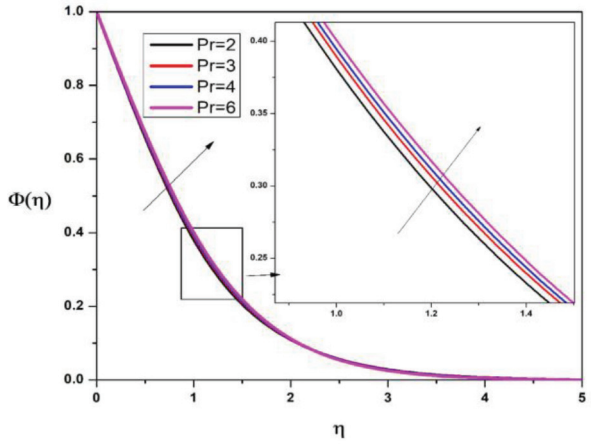


Figure 16. Plot of concentration Φ verses Prandtl number Pr.

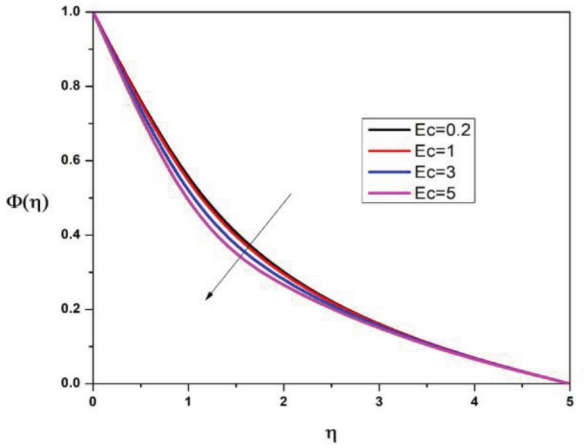


Figure 17. Plot of Concentration Φ verses Eckert number Ec.

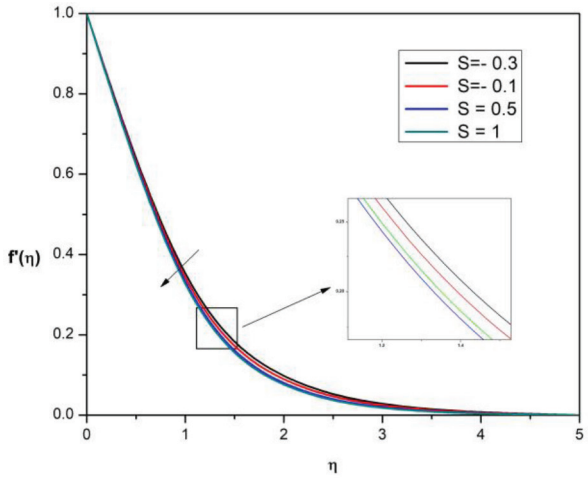


Figure 18. Plot of dimensionless velocity verses suction parameter S.

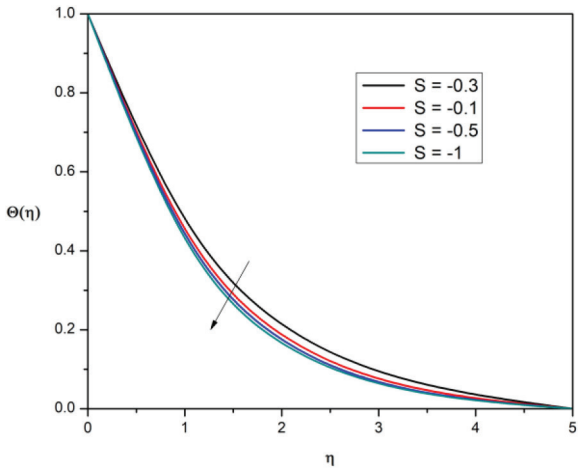


Figure 19. Plot of temperature θ verses Suction parameter S.

Figure 4 demonstrates the influence of the penetration parameter on concentration. With increase of the permeability factor there is increasing rate of concentration is owing to the fact that increasing the level of viscosity will decrease the flow of fluid thus the acceleration of the level of concentration will be gradually increasing.

The value of the concentration field for shifting Schmidt number (Sc) values is shown in Figure 5 The level of concentration of the fluid decreases with increasing Sc values, as seen in Figure 5. For high Sc levels, the rate of concentration decline is faster. Because higher levels of the Schmidt number correspond to lower mass diffusivity. As a result, the concentration profiles show a decreasing tendency.

The influence of Schmidt number Sc on temperature is seen in Figure 6. The temperature rises as the Schmidt number increases. The Schmidt number is a measure of the diffusivity of heat to mass diffusion ratio. The larger the Schmidt number, the greater the thermal diffusivity, and hence the higher the temperature profile.

The effect of the Dufur effect on heat is seen in Figure 7. The graphical findings indicate that when the Dufour force is increased, the temperature of the fluid rises, whereas the opposite behaviour is observed in the mass density. In the Figure 8. Increasing Du viscosity reduces concentration suspension and raises temperature, causing temperature to rise and concentration profiles to fall.

Figure 9 depicts the dimensionless velocity f' vs parameter A. If the parameter 'A', which signifies unsteadiness, is increased, the velocity decreases. A value of 'A' increase that depicts unsteadiness may induce a temperature decline due to greater heat transfer effects.

By disturbing the flow structure and the dispersion of the energy inside the pattern, velocity may be reduced.

The influence of Brownian motion on heat is seen in Figure 10. Brownian motion occurs in the nanofluid model owing to the presence of nanoparticles and affects the fluid's velocity and heat transmission characteristics. Brownian motion of nanoscaled particles increases the mobility and hence the thermal behaviour of the fluid flow.

Temperature is shown against parameter A in Figure 11. When the value of the variable 'A', which represents unsteadiness, is raised, the temperature drops. A value of 'A' increase that depicts unsteadiness may induce a temperature decline due to greater heat transfer effects.

Figures 12 and 13 show the impacts of Nb and Nt on concentration patterns for various parameter values, resulting in the widening of the nanofluids border concentration layer. On the nano fluid concentration boundary layer, Brownian motion exhibits reversal behaviour. Both friction factor values are shown to rise as the nanoparticle volume percentage increases. when a

Table 1. The skin friction coefficients for a number of parameters.

Pr	A	M	R	Ishak[23]	Saleem *et al.* [22]	Present Result
0.72	0	0	0	0.8086	0.80861	0.808612
1				1	1.00024	1.000241
3				1.9237	1.92361	1.923611
0.72	1	1	1	NA	0.70864	0.708642
1				NA	0.8678	0.86782
3				NA	1.6081	1.60814

Table 2. The Heat transfer rate coefficient for a number of parameters

Sc	Pr	Ec		R		Du	S	Nusselt no. Saleem *et al.*[22]	Nusselt no. (Present)	Sherwood number Saleem *et al.*[22]	Sherwoodnumber (Present)
0.5								0.14731	0.147311	0.20656	0.206566
1								0.14986	0.149863	-0.03305	-0.033051
1.5								0.1511	0.15112	-0.13568	-0.135685
	4							-0.68762	-0.687623	0.67507	0.675074
	8							-0.26558	-0.265581	1.04382	1.043822
	12							2.25205	2.252053	1.15988	1.15988
		0.5						-0.04382	-0.043822	0.22857	0.228573
		1						0.0859	0.08591	0.28849	0.288496
		1.5						0.21567	0.215674	0.34841	0.348414
			0.1					0.14757	0.147571	0.18064	0.180643
			0.2					0.10086	0.100863	0.19703	0.197032
			0.3					0.05304	0.053041	0.21353	0.213533
				0.5				0.11933	0.119335	0.22857	0.228571
				1				0.11035	0.110351	0.28849	0.288492
				1.5				0.09219	0.092196	0.34841	0.348413
					0.2			-	0.204575	-	0.354456
					0.4			-	0.200013	-	0.345568
					0.6			-	0.199355	-	0.333444
						0.1		-	0.251436	-	0.294578
						0.3		-	0.264587	-	0.306579
						0.5		-	0.273465	-	0.299945
							0.1	-	1.105448	-	0.226458
							0.2	-	1.000456	-	0.215487
							0.3	-	0.995454	-	0.201254

result, when the value of Nb increases, the concentration decreases. With larger values of the selected parameter, Nt appears to have an effect on increasing nanofluid concentration.

Figure 14 depicts velocity changes as a function of the magnetic parameter. From a physical standpoint, the presence of the magnetic field generates current inside the fluid flow domain, which produces resistance, causing the fluid's temperature to rise and its velocity to decrease owing to the Lorentz force.

The impact of the Prandtl number on fluid temperature is seen in Figure 15. The graph indicates that as Pr increases, so do the temperature fields. The observed behaviour in the fluid's temperature is accurate, based to the mechanics of the Prandntl number. The Prandtl number relates boundary layer's velocity to the radiative boundary layer by relating kinematic viscosity to thermal diffusivity. The greater the thermal diffusivity, the lower the Prandtl number.

The impact of the Prandtl number on fluid concentration is seen in Figure 16. The graph indicates that as Pr increases, so do the concentration fields.

The variation in Eckert number with intensity is seen in Figure 17. Concentration drops as the Eckert number increases. This is because the mechanical energy is transformed to thermal energy by the addition of the viscous dissipation effects Ec, which elevates the temperature of the fluid. As a result, the fluid thins, increasing its velocity while decreasing its mass concentration.

Figures 18 and 19 show how the suction parameter S affects the velocity profile and thermal boundary layer. The rising suction parameter S, where the velocity of the fluid is seen to rise with blowing, is noticed. When surface suction (S>0) is considered, the dimensionless velocity field diminishes and the edges of the layer thickness falls.

Table 1 shows the skin friction coefficients estimated for various values of Pr, A, M and R in absence of nanofluid and compared with Saleem *et al.*[22] and Ishak[23]. Table 2 compares the Nusselt number for various values of Pr, Sc, Ec, and R. Also, it shows present result for Du and S. The outcome is applicable to the current task.

4.0 Conclusions

We have investigated the effect of magnetohydrodynamic convective unsteady flow and heat transfer through a medium in the presence of drag force, suction/blowing, viscous dissipation and Dufur effect. The Governing equations are solved using shooting procedure with RKF45 Runge-Kutta Felhberg Method- Numerically. The effects of various parameters on the flow and heat transfer are observed from the graphs, and are summarized as follows:

- Velocity profile decreases with enhancement in magnetic parameter, M, A and S parameter since the flow is retarded by these parameters.
- Thermal boundary layer grows with Nb, Ec, Pr and Sc parameter while shows opposite behaviour with , Du and A parameter.
- Heat trasfer rate increases under the influence of Du while it decline with and Su.
- Improvement in concentration profile is visible for Pr and Nt parameter but reverse trend is observed with A, Ec, Nb, Du, and Sc parameter.
- The study sheds light on the migration of viscous nanomaterials like Metal (Al, Au, Cu, Fe, Ag), metal oxide (Al_2O_3, TiO_2, CuO), layered (Al+ Al_2O_3, Cu+C), carbon materials (graphite, CNTs, diamond) and nitride (AlN, SiN).

5.0 References

1. Sakiadis BC. Boundary-layer behavior on continuous solid surfaces: II. The boundary layer on a continuous flat surface. AIChE J. 1961; 7(2):221-5. https://doi.org/10.1002/aic.690070211
2. Crane LJ. Flow past a stretching plate. Zeitschrift für Angew Math und Phys. 1970; 21(4):645-7.
3. Choi SUS. Enhancing thermal conductivity of fluids with nanoparticles. Am Soc Mech Eng Fluids Eng Div FED. 1995; 231:99-105.
4. Buongiorno J. Convective transport in nanofluids. J Heat Transfer. 2006; 128(3):240-50. https://doi.org/10.1115/1.2150834
5. Crane LJ. Flow past a stretching plate. Zeitschrift für Angew Math und Phys. 1970; 21(4):645-7. https://doi.org/10.1007/BF01587695
6. Khan WA, Pop I. Boundary-layer flow of a nanofluid past a stretching sheet. Int J Heat Mass Transf. 2010; 53(11-12):2477-83. https://doi.org/10.1016/j.ijheatmasstransfer.2010.01.032
7. Makinde OD, Aziz A. Boundary layer flow of a nanofluid past a stretching sheet with a convective boundary condition. Int J Therm Sci. 2011; 50(7):1326-32. https://doi.org/10.1016/j.ijthermalsci.2011.02.019

8. Cortell R. Effects of viscous dissipation and radiation on the thermal boundary layer over a nonlinearly stretching sheet. Phys Lett A. 2008; 372(5):631-6. https://doi.org/10.1016/j.physleta.2007.08.005
9. Prasad KV, Santhi SR, Datti PS. Non-Newtonian power-law fluid flow and heat transfer over a non-linearly stretching surface. Appl Math. 2012; 03(05):425-35. https://doi.org/10.4236/am.2012.35065
10. Mukhopadhyay S, Ranjan De P, Layek GC. Heat transfer characteristics for the Maxwell fluid flow past an unsteady stretching permeable surface embedded in a porous medium with thermal radiation. J Appl Mech Tech Phys. 2013; 54(3):385-96. https://doi.org/10.1134/S0021894413030061
11. Srinvasulu T, Bandari S. MHD boundary layer flow of nanofluid over a nonlinear stretching sheet with effect of non-uniform heat source and chemical reaction. J Nanofluids. 2017; 6(4):637-46. https://doi.org/10.1166/jon.2017.1362
12. Jaafar A, Waini I, Jamaludin A, Nazar R, Pop I. MHD flow and heat transfer of a hybrid nanofluid past a nonlinear surface stretching/shrinking with effects of thermal radiation and suction. Chinese J Phys. 2022; 79:13-27. https://doi.org/10.1016/j.cjph.2022.06.026
13. Elgazery NS. Nanofluids flow over a permeable unsteady stretching surface with non-uniform heat source/sink in the presence of inclined magnetic field. J Egypt Math Soc. 2019; 27(1):9. https://doi.org/10.1186/s42787-019-0002-4
14. Jafar AB, Shafie S, Ullah I. MHD radiative nanofluid flow induced by a nonlinear stretching sheet in a porous medium. Heliyon. 2020; 6(6):e04201. https://doi.org/10.1016/j.heliyon.2020.e04201
15. Saeed A, Kumam P, Nasir S, Gul T, Kumam W. Non-linear convective flow of the thin film nanofluid over an inclined stretching surface. Sci Rep. 2021; 11(1):18410. https://doi.org/10.1038/s41598-021-97576-x
16. Rasool G, Shafiq A, Baleanu D. Consequences of Soret-Dufour effects, thermal radiation, and binary chemical reaction on Darcy Forchheimer flow of nanofluids. Symmetry (Basel). 2020; 12(9):1421. https://doi.org/10.3390/sym12091421
17. Abbas N, Rehman KU, Shatanawi W, Malik MY. Numerical study of heat transfer in hybrid nanofluid flow over permeable nonlinear stretching curved surface with thermal slip. Int Commun Heat Mass Transf. 2022; 135:106107. https://doi.org/10.1016/j.icheatmasstransfer.2022.106107
18. Khan SA, Hayat T, Alsaedi A, Ahmad B. Melting heat transportation in radiative flow of nanomaterials with irreversibility analysis. Renew Sustain Energy Rev. 2021; 140:110739. https://doi.org/10.1016/j.rser.2021.110739
19. Anwar MI, Ali M, Rafique K, Shehzad SA. Soret-Dufour and radiative aspects in hydromagnetized nanofluid flow in stratified porous medium. SN Appl Sci. 2019; 1(11):1430. https://doi.org/10.1007/s42452-019-1473-5
20. Reddy KV, Reddy MG, Reddy GR, Makinde OD. Analysis of joule heating and chemical reaction effects in electroosmosis peristaltic transport of couple-stress, micropolar and nanofluids. J Nanofluids. 2023; 12(3):796-808. https://doi.org/10.1166/jon.2023.1963
21. Ullah H, Fiza M, Khan K, Batool S, Ghufran SM, Al-Mekhlafi SM. Effect of joule heating and thermal radiation of MHD boundary layer Oldroyd-B nanofluid flow with heat transfer over a porous stretching sheet by finite element method. J Nanomater. 2022; 2022:1-11. https://doi.org/10.1155/2022/7373631
22. Saleem S, Nadeem S, Rashidi MM, Raju CSK. An optimal analysis of radiated nanomaterial flow with viscous dissipation and heat source. Microsyst Technol. 2019; 25(2):683-9. https://doi.org/10.1007/s00542-018-3996-x
23. Ishak A. Unsteady MHD flow and heat transfer over a stretching plate. J Appl Sci. 2010; 10(18):2127-31. https://doi.org/10.3923/jas.2010.2127.2131